Interpretation of cone pressuremeter tests to estimate the strain dependent stiffness and strength of sensitive lacustrine clay

Joshua Schorr[12#], *Stefan* Vogt[1], and *Roberto* Cudmani[1]

[1]*Technical University of Munich, Zentrum Geotechnik, Franz-Langinger-Street 10, 81245 Munich, Germany*
[2] *Boley Geotechnik GmbH, Auen Street 100, 80469 Munich, Germany (since November 2023)*
[#] *Corresponding author: j.schorr@boleygeotechnik.de*

ABSTRACT

Field and laboratory testing was carried out for the construction of a 100 m long cable stayed bridge situated in the foothills of the Alps in the south of Germany, a region dominated by deep post-glacial, fine-grained sediments. Due to the sensitivity and associated challenges with retrieving undisturbed soil samples in situ tests and their evaluation proved to be essential for the geotechnical design of the bridge foundation. This contribution focuses on the analytical and numerical interpretation of Cone Pressuremeter Tests (CPM). The non-linear G-γ relationship and undrained shear strength (using both the limit pressure and reverse plasticity contraction analysis) were determined analytically. Numerical investigations were carried out as verification using both the Finite Element method (FEM) using both 1D (cavity expansion) and 2D simulations (where the penetration of the probe was modelled) as well as using the Finite Difference (FD) method. 2D simulations demonstrated that the assumption of the cylindrical cavity expansion is appropriate for modelling the CPM tests. The interpreted undrained shear strength showed good agreement with other field tests, including CPTu, vane shear (FVT) and seismic cone penetration (SCPT) tests, as well as with the results of laboratory tests on disturbed samples. CPM tests with strain rate jumps were conducted during pressuremeter expansion, wherewith it was possible to quantify the viscous response of the soil. Based on the holistic interpretation of the field and laboratory results involving both numerical simulations and analytical methods the parameters for the material model Viscohypoplasticity were calibrated.

Keywords: Pressuremeter testing, sensitive clay, FE-modelling, non-linear shear stiffness, shear strength, viscosity

1. Background

1.1. Motivation

The design of the Mangfall bridge, a 100 m long cable-stayed bridge in the region of Rosenheim, situated approximately 100 km south-east of Munich, was particularly challenging due to subsoil conditions consisting of quaternary young sediments mainly of sensitive, soft, low-plastic, fine-grained lacustrine clay deposits (see Cudmani et al. 2022 & Rebstock et al. 2022). The characteristic propensity of the sediments to disturbance, i.e. a loss of their strength from fabric and bonding through both static and dynamic loading, mean that obtaining realistic geotechnical parameters from laboratory tests is significantly limited.

As a result of the sensitivity, undrained triaxial shearing on liner samples obtained using percussion drilling showed: (1) a ratio of $\Delta e/e_0$ of >14% following consolidation to estimated in situ stress, (2) a lower than expected preconsolidation stress and (3) a dilatant behaviour with no pronounced peak strength. As such, the expected increase in compressibility (collapse) or strongly contractive behaviour (with large increase in pore water pressure) for sensitive fine grained soils was not observed. Meaning that the design of the geotechnical limit and serviceability states using laboratory testing can lead to unconservative designs.

It is well-accepted that for such soils, the supplementary use of in situ testing is recommended. Allowing for not only a characterisation of the soil, but also, as shown in this paper, aiding the calibration of complex constitutive models — such as those describing non-linear shear strain dependent shear stiffness (G-γ). This paper focuses on the analytical and numerical interpretation of a field campaign featuring the cone pressuremeter (CPM) tests and on the assessment of the suitability and limitations of Viscohypoplasticity for modelling the behaviour of Rosenheim clay.

1.2. Cone pressuremeter

CPM tests were carried out using the so-called integrated cone penetrometer with a cross sectional area of 15 cm² and an angle of 60° (see Figure 1). The CPM is similar to the device described in DIN EN ISO 22476-08 and was manufactured by the company Cambridge Insitu Ltd. using the CPT cone from Fugro GmbH.

The system uses a Pressuremeter module with a length of 25 cm located 1.2 m above the piezocone consisting of a membrane surrounded by metal strips which is expanded radially whilst (ideally) maintaining axially symmetric deformation. The expansion is achieved through pumping pressurized gas into the

pressuremeter cell, whereby the pressure ψ and the radial displacement y at three equally spaced arms at mid-height by strain gauges is measured. The external diameter of the CPM probe was 47 mm, the diameter without the membrane was 38.7 mm and the thickness of the metal strips was 0.53 mm.

The CPM is of the pushed-in type (i.e. full displacement) and is generally considered as disturbed due to the large deformations that occur during the cone penetration, meaning that soil within a certain radius surrounding the probe is in or near the critical state ($\dot{\varepsilon}_v = 0$, $\dot{q} = 0$). In contrast to the more widespread self-boring pressuremeter (SBP) for which the disturbance before radial expansion is thought to be much smaller.

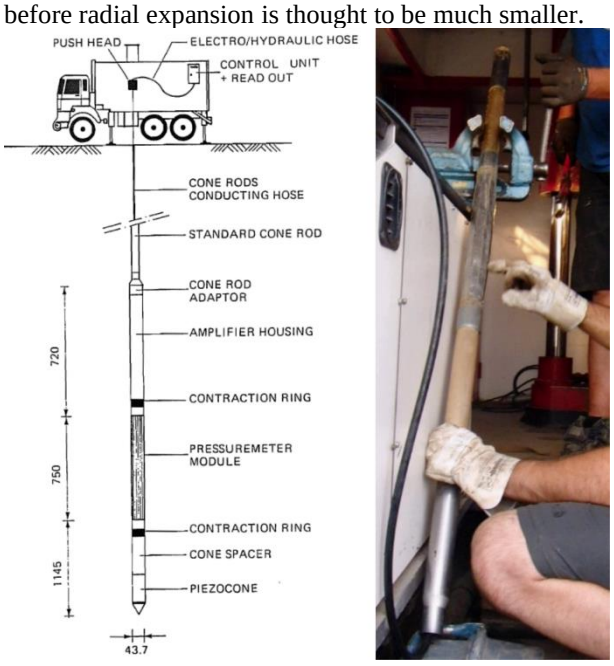

Figure 1. Left: Schematic depiction of the cone pressuremeter from Nutt (1993), and right: photo of the integrated CPM (from Cambridge Insitu / Fugro)

Though the response of the CPM is uncertain due to soil disturbance during installation, the varying high shearing rate, unknown drainage conditions, as well as regarding the inhomogeneous stress and strain path, analogous to CPT testing, CPM tests result in a repeatable amount of deformation, i.e. allowing for correlations.

Whilst usage of the CPM test has been limited due to the significantly higher cost than a CPT test, successful application has been documented in a wide variety of ground conditions, e.g. in a stiff over-consolidated clay (Houlsby & Withers 1988), the soft sensitive Bothkennar clay (Nutt 1993), in Lausatia Sand in the east of Germany (Cudmani & Osinov 2001), in over-consolidated till and in a sand deposit (Tucker et al. 2022).

1.2.1. Calibration

The radial displacements at the three arms are calculated from the voltage change of the strain gauges individually attached to each arm during the expansion and contraction. Conversion from Volts to mm is achieved through a zero shift and linear correlation factor. The gauges can measure a displacement of up to 9 mm comprising a full range accuracy of 0.1%. The inflation pressure was measured by a pressure transducer with a maximum capacity of 7 MN/m² at an accuracy of 0.5%. Due to the stiffness of the membrane a correction is made in respect to the recorded inflation pressure, based on an expansion in air ($\psi \approx 165$ kN/m² is reached at $y = 8$ mm). At higher pressures (i.e. not relevant for soft clay) the stiffness of the overall pressuremeter system (compliance) should be accounted. For the tests documented in this contribution, a linear correction factor of around 7 mm/GPa was determined.

1.3. Literature review

1.3.1. Introduction

A significant amount of research has been undertaken towards the end of the 20th century on the interpretation using analytical and numerical models based on the cavity expansion theory (e.g. Palmer 1972; Houlsby & Withers 1988; Yu 1990; Te & Houlsby 1991; Bolton & Whittle 1999; Cudmani & Osinov 2001, Osinov & Cudmani 2001; and Schnaid 2009). Generally, these models assume a radial expansion towards a homogeneous, isotropic, soil continuum, thus providing an attractive alternative to purely empirical correlations since the output of the correlation procedure are parameters quantifying the constitutive behaviour of the soil and the corresponding state variables. During penetration of the cone, the spherical and cylindrical expansion theory has been shown to be applicable for determining the soil state at the cone tip and at a location far behind the cone respectively (Te & Houlsby 1991). For the interpretation of CPM tests the latter is thought to be more appropriate (Nutt 1993).

1.3.2. Interpretation of the undrained soil response by analytical models

Most models for the interpretation of clays under undrained loading consider an isotropic, linear elastic-perfectly plastic constitutive model, such as the well-known result from Gibson (1961) based on the solution of the equilibrium equation at the boundary between the elastic and plastic region and the cavity wall, which at the limit pressure ($\Delta V/V \to \infty$) leads to:

$$\psi_L = \sigma_{h0} + c_u[1 + \ln(G/c_u)]. \quad (1)$$

Analogous to the approach by Palmer (1972), Houlsby (1988) showed that for a CPM test, c_u can be more reliably interpreted from the contraction phase. This interpretation assumes that the plastic soil region behaves initially elastically during unloading until the undrained strength of the material is reached at the cavity wall with $\sigma_r - \sigma_\theta = -2c_u$ and a reversal of the principal stress direction.

Numerous studies (Houlsby & Withers 1998; Nutt 1993; Jardine 1992; Bolton & Whittle 1999) have shown that the non-linear shear modulus can be interpreted from unloading-reloading cycles assuming that the condition of reverse plasticity is not reached, as opposed to the initial loading where the size of the plastic zone is increasing and where the extent of soil disturbance is unknown. It was demonstrated by Houlsby (1998) that the measured shear modulus is dominated by the shear stiffness of the soil in the near field surrounding the

cavity expansion and as such, the measured displacement at the cavity wall can be used to interpret the non-linear shear modulus of the soil. Based on work by Wood (1990) it was shown that the tangent modulus G_t can be calculated from the secant shear modulus G_s which is related to the pressiometer tangent modulus G_{pt} through:

$$G_t = G_s + \varepsilon_q \, \mathrm{d}G_s/\mathrm{d}\varepsilon_q \rightarrow G_{pt} = G_s = \mathrm{d}\psi/2\mathrm{d}\varepsilon_c \qquad (2)$$

with $\varepsilon_c = \ln[(r_0 + y)/r_0]$.

1.3.3. Interpretation by numerical models

Several numerical models for the interpretation of pressuremeter tests have been developed. Cudmani & Osinov (2001) used the finite difference method to simulate either the spherical or cylindrical cavity expansion, Yu (1990) developed a finite element code to perform 1D simulations (see also Nutt 1993, who investigated CPM tests in calcareous sands), and Aubeny et al. (2000) used the strain path method to model the installation of pressuremeters like the CPM, as probes fully radially displacing the soil while penetrating axially. However, to the Authors knowledge, no simulations considering both the push-in installation of the probe and the subsequent radial expansion of the CPM membrane have been carried out so far. The simulations reported in this contribution consider not only the coupled mechanical soil behaviour with the pore water response, but are also carried out using Viscohypoplasticity, a material model capable of capturing rate-dependent effects resulting from soil viscosity and the non-linear shear, whilst distinguishing between loading, unloading and reloading.

2. Rosenheim lacustrine sediments

2.1. Geological and site description

The region around the south German city of Rosenheim lies in the catchment area of the Inn River, which in the last ice age formed a part of a huge glacial valley termed the Ur-Inn. The glacial valley consisted of a solid ice layer at the base of the Alps surrounded by a terminal moraine barrier, resulting from debris or till, pushed by the advancing glacier. Following the end of the last ice age, the moraine dammed the meltwater of the glacier to form the so-called former 300 km² Rosenheim Lake, which filled over time with fluviatile sediments transported by the Inn. Depending on the flow velocity, fine-grained soils consisting of silt, clays and fine sands were deposited, which were estimated by Reich (1955) based on geophysical measurements to have thicknesses of up to 300 m.

Schumann (1969) proposes that the distinctive varved layers with visibly recognisably coarser-grained fine sands (see Figure 2) correspond to summer and winter sedimentation phases, with the layers formed during summer appearing to be lighter, and with a higher content of $CaCO_3$ (5-10%) as well as a higher water content compared to layers formed by sedimentation during winter. It is hypothesized that interparticle bonding by $CaCO_3$ concretions allow the soil structure to support higher water contents by creating a metastable fabric, which may become unstable due to external loading, and especially during alternating shearing. The moderate sensitivity (S_t of 4-6) estimated from vane shear tests are likely to be underestimated due to sample disturbance.

Figure 2. Close up of a sample of Rosenheim lacustrine sediments indicating layering

2.2. Soil classification

Classification tests on samples (generally using percussion core drilling, diameter of 180 mm) from a number of sites within the region of Rosenheim show a clay of low to medium plasticity (see Figure 3), void ratios of e = 0.9 to 1.1, a water content in the range of w = 30% to 50% and a liquidity index of about LI ≈ 1. With I_p = 10-20% the sediments are expected to behave as a clay (Boulanger 2006), with only some samples falling into the clay-like to sand-like behaviour (7% > I_p 3%).

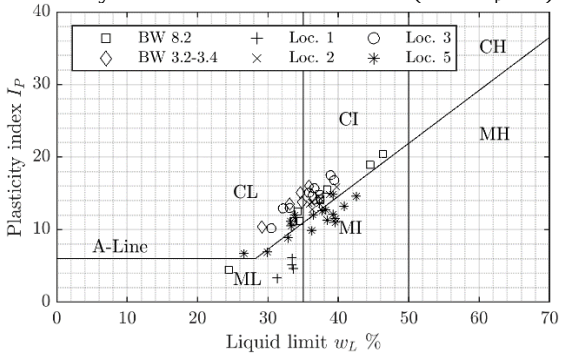

Figure 3. Plasticity chart

Little variation is observed across the different investigated sites within the Rosenheim region, meaning that field tests (e.g. SCPT tests) from neighbour sites can be assumed to be representative for the site of the cable-stayed bridge. The results regarding the soil composition also appeared to be comparably constant over the depth of drillings. Grain size distributions show clay contents of roughly 25-35%, with the remainder of the soil mass corresponding to roughly equally to fine- and coarse-grained silts.

2.3. CPT results

CPTu tests from the location where the CPM tests were carried out are shown in Figure 4, revealing predominantly a clay-like, contractive and sensitive SBT CCS. Isolated layers with the SBT CC can be observed, which correspond to slightly increased penetration resistance, increased F_r, and lower u_2. In more shallow depths, more sand-like dilative behaviour may be expected by the evaluation of the SBT.

Interpretation of the CPTu results was carried out by applying the three methods proposed in Karlsrud et al. (2005) with the factors N_{kt}, $N_{\Delta u}$, and N_{ke} using q_t, u_2 and B_q (see Figure 4). With N_{kt} = 9.5 estimated from

Karlsrud et al. (2005) using I_p = 15% and OCR = 1.5, the ratio c_u/σ_{v0} = 0.36 to 0.46 was found.

The assessment of layers of comparably high permeability was confirmed from pore water dissipation tests holding the CPTu cone in position at a certain depth while monitoring the decay of u_2. Based on the results of monotonous dissipation tests, a coefficient of permeability of $k_h = 10^{-9}$ to 10^{-8} m/s and a time to 50% dissipation of $t_{50} > 100$ s were estimated, indicating that partial drainage effects can be neglected by the evaluation of the CPTu results.

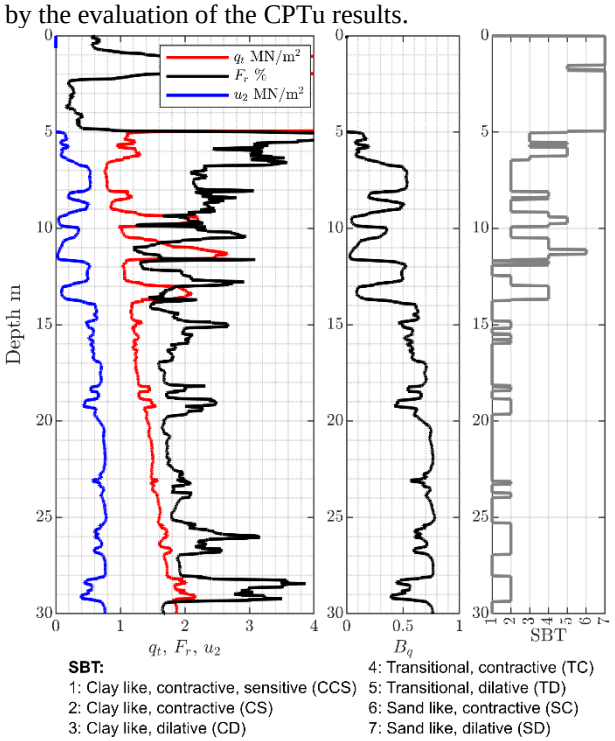

Figure 4. Typical CPT profile; net cone resistance q_t, normalised friction ratio F_r, dynamic pore water pressure u_2 profiles, excess pore water pressure ratio B_q and the soil behaviour type (SBT) according to Robertson (2016)

3. CPM tests at the cable-stayed bridge

As part of the site investigation campaign CPM tests were carried out at three different locations: two of the main pylons (A20 and A30) and at the site of pile loading testing (Aicherpark, see Cudmani et al. 2019). With the aim of quantifying the soil viscosity (i.e. creep and rate dependency), the following CPM tests were carried out: constant deformation rate of 0.15 mm/min with two unloading-reloading loops (Type 1), constant deformation rate of 0.15 mm/min up to the limit pressure followed by 10x increase in the deformation rate (Type 2), constant rate of 0.15 mm/min with creep tests (Type 3), and combinations of Type 1 and 2 (see Figure 5).

For the interpretation of the pressuremeter results, the initial horizontal stress was calculated from the relationship $\sigma'_{h0} = \sigma'_{v0} \cdot K_0$ with $K_0 \approx 0.55$ based on a $I_p \approx 20\%$ (Massarsch 1979).

3.1. Analytical interpretation

3.1.1. Viscosity index

Assuming an undrained expansion, the viscosity was evaluated using the relationship by Scherzinger (1991) for the so-called viscosity index (proportionality between stress and strain rate) of:

$$I_v = \ln(q_1/q_2)/\ln(\dot{\varepsilon}_1/\dot{\varepsilon}_2) \quad (3)$$

where $q = 2 \cdot c_u = \sigma_r - \sigma_\theta$, $\dot{\varepsilon}$ is the strain rate and subscript i refers to different strain rates.

In the tests, the limit pressure ψ_L was generally not reached. Thus, I_v was assessed visually by calculating ψ_1 corresponding to a constant strain rate of $\dot{\varepsilon}_{c,1}$ = 0.15 mm/min based on Eq. 3 (where q can be replaced by ψ and the cavity strain $\dot{\varepsilon}_c$ is used), based on the measured ψ_2 and $\dot{\varepsilon}_{c,2}$. This normalisation is shown in Figure 5, where a low to medium degree of viscosity I_v = 0.02 was found to give a good agreement with the data (i.e. influence of the strain jump was eliminated).

3.1.2. Strain dependent shear modulus

The non-linear shear modulus was determined from Eq. 2 considering the unloading-reloading loops. To enable comparison with conventional laboratory testing the tangent CPM shear modulus G is plotted with the secant shear strain γ $(= \varepsilon_r - \varepsilon_\theta \approx -2\varepsilon_c)$, which was calculated as the difference between a reference strain γ_{ref} equal to the strain at the start of the unloading or reloading loop and the current strain.

The tangent CPM stiffness $d\psi/2d\varepsilon_c$ was calculated numerically using the centred divided difference method, considering a step size of h = 2. The unloading-reloading loops for each test were analysed, where the following was observed: (1) all unloading loops where comparable regarding the quantity and change of stiffness modulus, (2) no systematic increase in stiffness (i.e. undrained condition holds) with slightly increasing cavity deformation at the onset of unloading, and (3) stiffness modulus during reloading showed significantly more scatter than during loading.

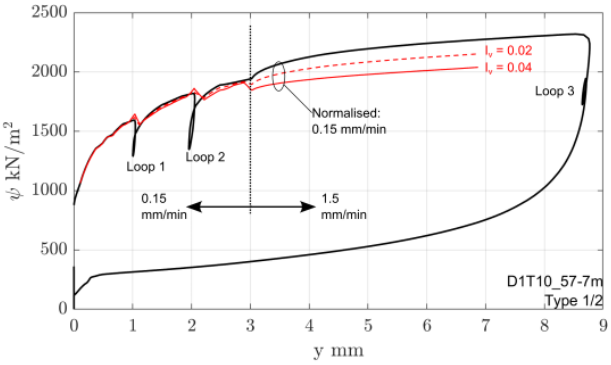

Figure 5. Radial expansion of the membrane y over inflation pressure ψ for a test of Type 1/2 with three unloading-reloading loops (black line) and normalized ψ using expansion rate of 0.15 mm/min (red lines); 10-fold increase after y = 3 mm

The G-γ relationship was determined from the unloading using the relationship by Darendeli (2001):

$$G = G_0/[1 + (\gamma/\gamma_{ref})^\alpha], \quad (4)$$

where for each test, the parameters G_0, γ_{ref} and α were fitted using the method of least squares. The fitted G_0 (termed $G_{max,CPM}$) generally lies between the upper $G_{max,upp}$ and lower $G_{max,low}$ bounds of the shear modulus at very small strains interpreted from SCPT tests (see

Figure 6 (a)). Based on this agreement the curves were normalised by $G_{\max,avg}$ (average of $G_{\max,upp}$ and $G_{\max,low}$) and a single value for γ_{ref} and α was fitted (see Figure 6 (b)), i.e. a single G-γ curve was determined.

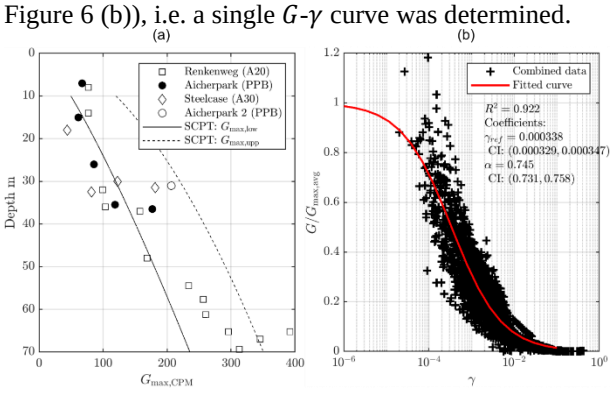

Figure 6. (a) Comparison of G_{max} obtained from CPM tests with SCPT tests, and (b) fitted non-linear shear modulus

3.1.3. Undrained shear strength

Figure 7 highlights the estimations of c_u by the CPM tests compared to the results of CPT and FVT tests, as well as undrained triaxial compression tests under both isotropic (CIU) and K_0 consolidation (CK_0U). The empirical N_{kt} approach from Karlsrud et al. (2005) shows an excellent agreement with the values of c_u derived from CPM tests using ψ_L (solution to Eq. (1) with $G_{0.2\%}$).

A pronounced anisotropy was observed, along with the contraction phase (reverse plasticity) of the CPM test revealing a 20-30% lower c_u (comparable with FVT).

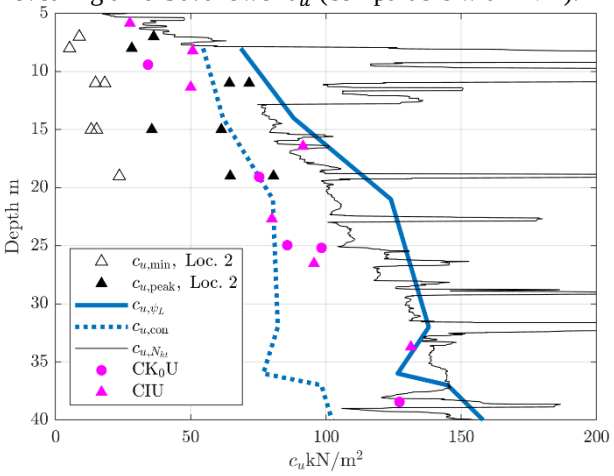

Figure 7. Comparison of undrained shear strengths obtained from CPM tests during expansion (c_{u,ψ_L}, using estimated limit pressure) and during contraction ($c_{u,con}$) with those from vane shear tests (max. and res. Strength with filled and empty symbols respectively), CPT tests ($c_{u,N_{kt}}$) and from undrained triaxial compression tests with disturbed samples (CK_0U / CIU)

3.2. Numerical interpretation

3.2.1. Viscohypoplasticity

Numerical simulations were performed using the material model of Viscohypoplasticity from Niemunis (2003). The constitutive equations are consistent with the compression model by Butterfield (λ and κ), as well the widely used Isotach model (Leroueil & Vaughan 1990) for predicting the effects of soil viscosity as rate dependency, creep and relaxation. The small-strain stiffness is considered by the material model featuring the intergranular strain concept (Niemunis 2003). This constitutive model does not capture the influence of the structure on the stiffness and the shear strength. During monotonic undrained shearing the model predicts an increase of the shear resistance towards the critical state, rather than the for sensitive soils expected peak resistance followed by a pronounced softening.

The material parameters of the viscohypoplastic model shown in Table 1 were calibrated based on simulations of laboratory tests on disturbed soil samples and measurements from a trial embankment. Representing therefore, an intermediate stage between disturbed and the undisturbed subsoil conditions. Based on the interpretation of the field tests, an OCR of 1.5 was adopted which is in agreement with the expected slightly overconsolidated state based on the estimated geological age, due to creep and diagenesis.

Table 1. Calibrated material parameters Viscohypoplasticity

e_r	υ	λ	κ	β_R	I_v	D_r	φ_c
0.86	0.2	0.04	0.005	0.5	0.02	10^{-7} s^{-1}	30°

	m_T	m_R	R	β_χ	χ
Intergranular strain parameters:	5	5	10^{-4}	0.3	0.5

3.2.2. 1D Cavity expansion (undrained)

To verify the analytically obtained $G_{0.2\%}$ (shear modulus corresponding to γ of 0.2% or a rigidity index of I_R = 500) and c_{u,ψ_L} linear elastic perfectly plastic undrained (i.e. ν = 0.49) simulations of a cylindrical cavity expansion were performed using ABAQUS (Dassault Systèmes, 2017) with quadratic 9-node elements. Based on Figure 6 (b) G is not expected to vary significantly within the expected range of I_R = 200 to 500. The comparison in Figure 8 shows a good agreement with test results, aside from initially due to the assumed strong influence of soil disturbance. Anisotropy of the soil during the unloading is observed as FE simulation show steeper gradient compared to the test data.

Cylindrical cavity expansion simulations using Viscohypoplasticity with the 1D FE model and the Finite Difference Model (FDM) from Cudmani & Osinov (2001) are shown in Figure 9 for a single test (above). Comparison for test D1T03 reveals a slight underprediction of ψ. The unloading-reloading behaviour appears to be reproduced accurately by both the FE and FD simulations.

The estimated ψ_L for each test are shown in Figure 9 (below), which could be described by a linear relationship with the depth (z). The FDM simulations performed at different depths using the calibrated material parameters from Table 1 show a good agreement with $\bar{\psi}_L$. It appears that the undrained shear behaviour of the soil disturbed by the installation of the pressuremeter can be realistically captured using visco-hypoplasticity, although the undisturbed initial state of the soil was assumed in the simulation of the cavity expansion. This apparently contradictory finding can be explained as follows: Push-in installation is expected to damage the soil structure (reduce shear resistance) and induce an increase of the mean effective stress (increased shear

resistance) around the pressuremeter. If during the pressuremeter expansion, these mutual effects nearly cancel each other out, the pressuremeter expansion will correspond to the wish-in-place conditions.

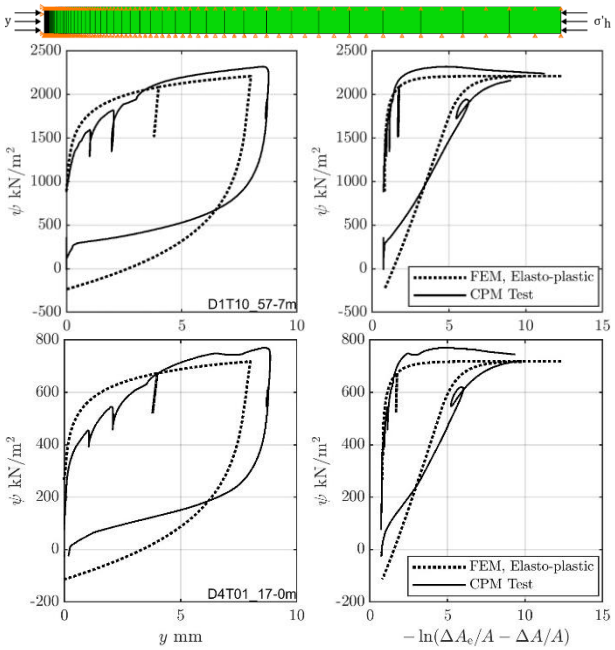

Figure 8. Illustration of the 1-D FE model (above) and representative results of the elasto-plastic FE-simulations (undrained) using $G_{0.2\%}$ and c_{u,ψ_L}(below)

In Figure 10, the shear modulus determined from cyclic simple shear (SS) element test simulations (black, with symbols) are compared with the analytical interpretation using Eq. 2 (red) and the 1D FE cavity expansion simulation (dotted and dashed black line) considering the calibrated parameters for β_χ and χ (Table 1). The shear modulus from the CPM (experimental and calculations) are normalised by the $G_{\max}$ from the SS simulation, which reveal generally a good agreement between the analytical interpretation and the numerical solution. A deviation between the analytical and numerical result is only evident in the small strain range ($\gamma < 5{\cdot}10^{-4}$). This limitation can be attributed to the accuracy of the radial displacement measurement in the pressuremeter cell and the stronger influence of the membrane stiffness correction for small pressure changes.

3.2.3. 2D Cone penetration (coupled simulations)

To assess the influence of the cone penetration and whether the assumption of a cylindrical deformation field holds, 2D simulation coupled (mechanical-pore water) simulations were carried out using the model represented by Figure 11. A penetration of 1 m at a rate of 2 cm/s was simulated to ensure steady state conditions were reached. Simulation results of the penetration considering a permeability of $k_h = 10^{-9}$ m/s estimated from dissipation tests are shown in Figure 12.

To ensure numerical stability by limiting excessive distortion of the mesh during axial penetration, these simulations considered only the displacement of the soil due to the cone, with a frictionless contact between the cone and the soil. The influence of friction at the cone was assessed based on a single undrained simulation with a simple constitutive model assuming a Coulomb law with μ = 0.2 which resulted in comparable pore water pressure and tip resistances (until early termination due to convergence issues). For the simulations without friction the correction procedure described by Meier (2007) was applied.

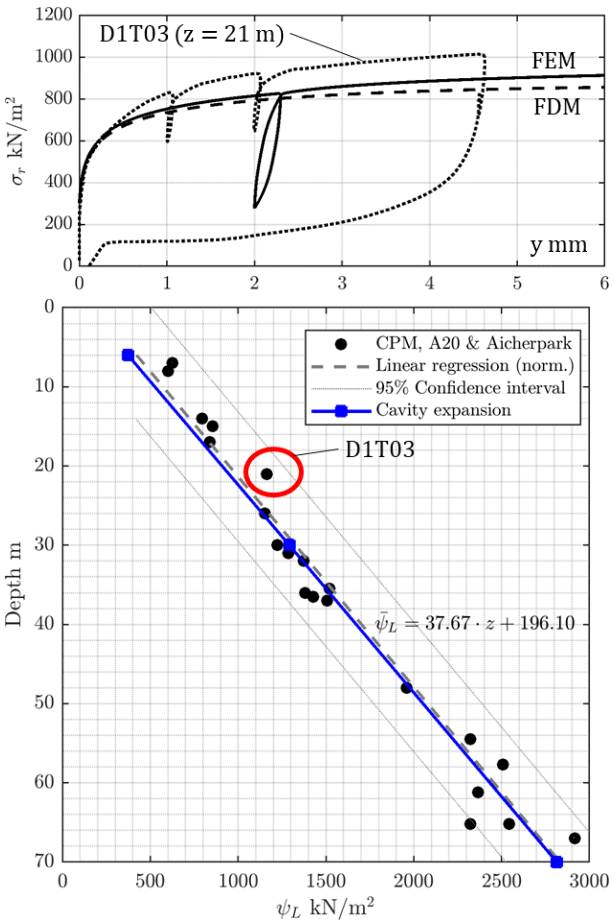

Figure 9. Comparison of test results with FDM and FEM simulations using Viscohypoplasticity (above) and determined linear increase of ψ_L with increasing depth hence effective stress (below)

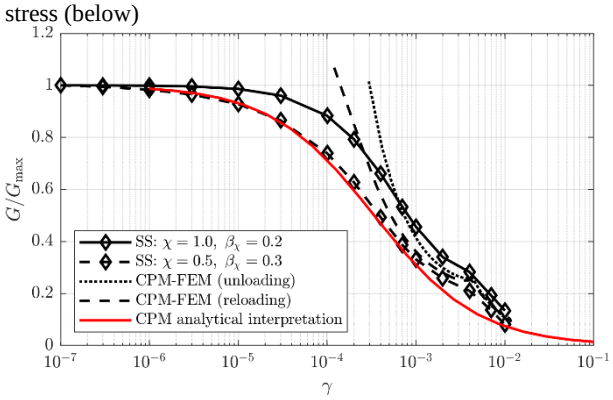

Figure 10. Simple shear (SS) and 1D CPM FEM simulation results (black, using Viscohypoplasticity) vs. analytical interpretation (red)

Figure 12 show large deviatoric stresses surrounding the cone tip within a roughly a circular influencing zone of a radius of about 3D to 5D. Furthermore, a significant unloading is observed at the soil "behind" the cone shoulder, as suggested by literature. However, the final horizontal pressure is still significantly larger than the initial in situ stress.

The comparison of the calculated and measured cone resistance at different depths in Figure 13 reveals in accordance with the reality, a linear dependence of the tip resistance on the effective stress, but the tip resistance is overestimated by around 50%. This results most probably from the decay of the soil structure of the sensitive soil and confirm the observation by Cudmani et al. (2022) reporting that resistance during the cone penetration test is reflecting likely the disturbed state of soil. As shown in Figure 13, to roughly consider the actual decay of soil resistance during penetration and obtain a better agreement of calculated and measured cone resistances without changing the model parameters, the initial void ratio was artificially increased from the actual values corresponding to $OCR = 1.5$ to values corresponding to $OCR \approx 0.8$.

The calculated and measured dynamic pore water pressure at the shoulder of the cone, which are mainly resulting from the undrained compression near the tip and only to a minor extent from shearing, show a good agreement.

3.2.4. 2D Membrane expansion

The expanding membrane of the pressuremeter module of the CPM was modelled using 2D linear axisymmetric membrane elements (MAX1) in Abaqus (see Figure 11) allowing for a realistic simulation of the radial expansion phase of the inflation. In Figure 14, the results of two FE-simulations assuming undrained and partially drained conditions with an increased permeability to approximate a fully drained expansion are compared with the results of the corresponding CPM test and the 1D cavity expansion solution.

It is evident that the total radial stresses recorded at the mid and top position show little differences between the drained and undrained expansion, but the effective stresses to mobilize a given radial deformation are considerable higher during the drained expansion.

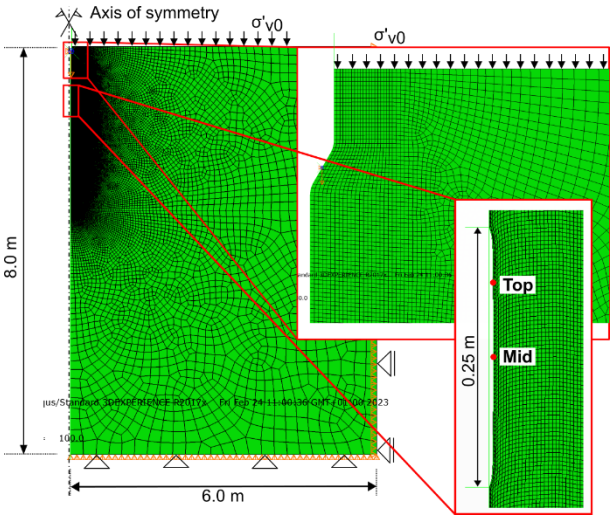

Figure 11. 2D FE model of the simulation of CPM tests with B.C. shown schematically (left); FE mesh at the tip of the cone including the phase of pre-deformation (above right); and deformed mesh surrounding pressuremeter module following inflation (insert bottom right)

Furthermore, the comparison of the calculated cavity expansion response for the push-in and wished-in-place installation shows a difference in the total radial stress $\Delta\sigma_r$ with larger values for the push-in installation. As it can be inferred from Figure 14, the value of $\Delta\sigma_r$ corresponds approximately to the difference between the initial total radial stress at the beginning of the cavity expansion, which is higher for the push-in than the wish-in-place installation (in Figure 14, $\Delta\sigma_r \approx 300\ kPa$). The larger limit pressure for the push-in installation in comparison to the wish-in-place installation results from the increase of effective stress induced by the pushed-in installation.

As observed in Figure 13 for the cone resistance, the numerical model considering the push-in installation overestimates the actual radial pressure required to expand the pressuremeter. This results from an overestimation of the increase of effective stresses induced by push-in installation. As explained in section 3.2.3, this can be attributed to the actual decay of structure in the sensitive soil during push-in installation, which cannot be captured by the used constitutive model.

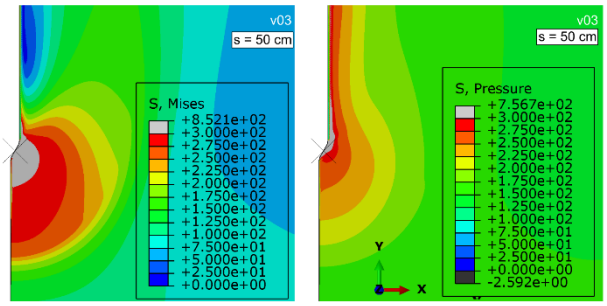

Figure 12. Contours of the Von Mises deviatoric stress and mean effective pressure after 50 cm of axial penetration (depth, z = 20 m)

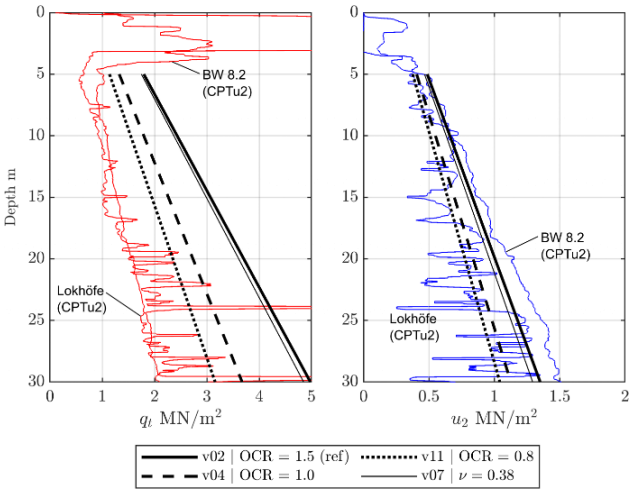

Figure 13. Results from the 2D FE model of CPM installation and expansion.

4. Conclusions

The CPM test is a powerful tool for the in situ characterisation of low plastic fine-grained sensitive lacustrine clay. The test enables not only the estimation of c_u based on the theory of cavity expansion as opposed to relying on empirical correlations but can also be used to estimate the strain dependent G-γ relationship.

Furthermore, the soil anisotropy was assessed based on the analysis of the contraction phase during CPM testing, revealing a reduction in c_u of 20-30%.

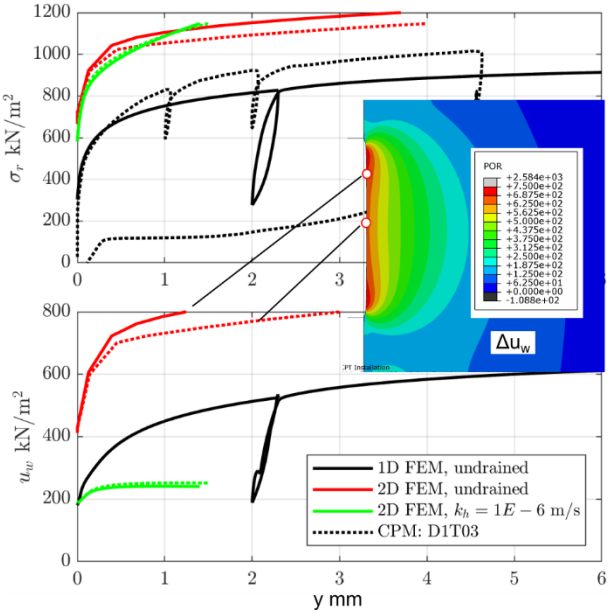

Figure 14. Comparison of 1D and 2D simulations including the simulation of the installation process with test results from CPM

For the case of the examined sensitive lacustrine sediments, the push-in installation induces on the one hand an increase of the mean effective pressure, on the other hand a reduction of stiffness and strength in the sensitive soil surrounding the probe due to a decay of the structure. Therefore, the proposed numerical model, which can capture only the increase of the effective stress, but not the decay of the structure of the sensitive soil, overestimates the CPM limit pressures.

In addition, we observe that our numerical model can realistically predict the CPM results by assuming a wish-in-place installation. This would indicate that in our case the mutual effects described above cancel each other out.

A similar conclusion can be drawn from the comparison of the simulated and measured cone resistance, which also shown an overestimation of the measured values. This is also caused by the inability of the numerical model to capture the influence of the soil structure on the evolution of the shear resistance during penetration.

Acknowledgements

The work was carried out by the Technical University of Munich, Zentrum Geotechnik (TUM-ZG). Discussions with Daniel Rebstock and Cambridge Insitu Ltd. are gratefully acknowledged, as is the contribution of Michael Niebler (TUM-ZG) to the modelling of the membrane.

References

Aubeny, C., Whittle, A. and Ladd, C. “Effects of Disturbance on Undrained Strengths Interpreted from Pressuremeter Tests”, In: J Geot and Geoenv Eng, 126(12), pp. 1133-1144, 2001. http://doi.org/10.1061/(ASCE)1090-0241(2000)126:12(1133).

Boulanger, R.W. and Idriss, I.M. “Liquefaction Susceptibility Criteria for Silts and Clays”, in: J Geotech Geoenv Engrg, 132(11), pp. 1413-1426), 2006, https://doi.org/10.1061/(ASCE)1090-0241(2006)132:11(1413)

Bolton, M. D. and Whittle, R. W. “A non-linear elastic/perfectly plastic analysis for plane strain undrained expansion tests”, in: Géotechnique, 49(1), pp. 133-141, 1999.

Cudmani, R and Osinov, V. “The cavity expansion problem for the interpretation of cone penetration and pressuremeter tests”, In: Can Geot J 38, pp. 622-638, 2001. 10.1139/cgj-38-3-622, http://doi.org/10.1139/cgj-38-3-622.

Cudmani, R., Rebstock, D., Schorr, J. „Geotechnical Challenges for the Numerical Prediction of the Settlement Behaviour of Foundations in Rosenheim’s Seeton”, In: Triantafyllidis, T. (eds) Recent Developments of Soil Mechanics and Geotechnics in Theory and Practice. Lecture Notes in Applied and Computational Mechanics, vol 91. Springer, Cham., 2020, https://doi.org/10.1007/978-3-030-28516-6_17.

Cudmani, R., Premstaller, M., Rebstock, D., Vogt, S. “Geotechnische in situ Charakterisierung von Seeton am Beispiel des Rosenheimer und Salzburger Beckens“, („Geotechnical in situ characterisation of Seeton using the example of the Rosenheim Salzburg deposits” in German), 36. Christian Veder Kolloquium, Technical University of Graz, Graz, June 2022.

Dassault Systèmes, Finite Element Program: ABAQUS 2017 documentation, 2017.

Darendeli, M. B. “Develoment of a New Family of Normalized Shear Modulus Reduction and Material Damping Curves”. Ph.D. Diss, The University of Texas, Austin, Texas, 2001.

Houlsby, G. and Withers, N. “Analysis of the cone pressuremeter test in clay” in Geotechnique, 38(4), 1988, pp. 575-587, https://doi.org/10.1680/geot.1988.38.4.575.

Jardine, R. J. “Nonlinear stiffness parameters from undrained pressuremeter tests” in: Can Geot J, 29(3), 1992, pp. 436-447.

Karlsrud, K., Lunne, T., and Strandvik, S. “CPTu correlations for clays”, In: Geotechnology in Harmony with the Glob Env, 2005, pp. 693-702. IOS Press BV.

Leroueil, S. and Vaughan, P. R. “The general and congruent effects of structure in natural soils and weak rocks” In Géotechnique, 40(3), 1990, pp. 467-488, https://doi.org/10.1680/geot.1990.40.3.467

Massarsch, K. R. “Lateral earth pressure in normally consolidated clay”, In: 7th Europ Conf Soil Mech Found Eng, 1979, pp. 245-249, Brighton, UK.

Meier, T. “Application of Hypoplastic and Viscohypoplastic Constitutive Models for Geotechnical Problems”. Phd dissertation, Universität Fridericiana zu Karlsruhe, Karlsruhe, 2007.

Niemunis, A. “Extended Hypoplastic Models for Soils”, Habilitation Thesis, Band 34, Institute für Grundbau und Bodenmechanik der Ruhr-Universität Bochum, 2003.

Rebstock, D., Schorr, J., Cudmani, R., Kegl, K. „Beurteilung der Messergebnisse der Gründungen einer Schrägseilbrücke in Rosenheimer Seeton“, („Assessment of the monitoring results of the foundations of a cable-stayed bridge in Rosenheim“ in German), 36. Christian Veder Kolloquium, Technical University of Graz, Graz, June 2022.

Reich, H. „Senkung des bayerischen alpenvorlandes“, („Sinking of the foothills of the Bavarian Alps“ in German) Naturwissenschaft Rundschau, 8, 1955, pp- 150-154.

Schumann, W. „Geochronologische Studien in Oberbayern auf der Grundlage von Bändertonen“ („Geochronological studies in upper Bavaria on the basis of varved clay” in German). Verlag der Bayerischen Akademie Der Wissenschaften, 1969.

Wood, D.M. “Strain dependent moduli and pressuremeter tests” in Géotechnique, 40(3), 1990, pp. 509-512.

Yu, H. S. “Cavity expansion theory and its application to the analysis of pressuremeters,” PhD thesis, Oxford University, Oxford, England, 1990.